

Application of focused ion beam technology for fabrication of photonic nanostructures

Feridun Ay, Vishwas J. Gadgil, Dimitri Gekus, Shanmugam Aravazhi, Kerstin Wörhoff,
and Markus Pollnau

Integrated Optical MicroSystems Group, MESA+ Institute for Nanotechnology,
University of Twente, P.O. Box 217, 7500 AE Enschede, The Netherlands, V.J.Gadgil@utwente.nl

ABSTRACT

We report our recent results on focused ion beam (FIB) nano-structuring of Bragg gratings in both, amorphous Al_2O_3 and crystalline $\text{KY}(\text{WO}_4)_2$ channel waveguides. By optimizing FIB milling parameters such as ion current, dwell time, loop repetitions, scanning strategy, and improving sidewall definition, reflection gratings with smooth and uniform sidewalls are achieved. The redeposition effects are significantly reduced and gratings more than $4\ \mu\text{m}$ in depth with an improved total sidewall angle of about 5° are achieved by varying dwell time and pixel resolution distribution for the same dose per area.

Keywords: focused ion beam nanostructuring, optical waveguides, photonics, gratings.

1 INTRODUCTION

Focused Ion Beam (FIB) processing is an emerging tool in nanotechnology [1]. It has been used extensively in failure analysis in the semiconductor industry. FIB milling enables fast, reliable and well-controlled nanometer-size feature definition. Since the method involves physical removal of material by a beam of ions, the technique can be adapted and optimized almost for any material system [2,3]. Structures can be directly written on a substrate instead of having to follow the expensive and time consuming route of photolithography.

In this report, a case study on the fabrication of integrated Bragg gratings to form on-chip optical cavities is presented. We discuss strategies to optimize the nano-structuring processes that are strongly dependent on the geometry of the desired structure. Furthermore, we report our recent results on utilization and optimization of the FIB technique for

the fabrication of nano-structures in integrated photonic devices on several material platforms, such as amorphous Al_2O_3 and crystalline $\text{KY}(\text{WO}_4)_2$ (or KYW).

Both, Al_2O_3 and KYW are promising materials for photonic applications with excellent optical properties and of interest for obtaining on-chip resonator structures. The monoclinic KYW is recognized as an excellent host material for rare-earth ions, providing high absorption and emission cross sections, especially when doping it with Yb^{3+} [4]. Recently, laser emission with slope efficiencies up to 82.3% has been obtained in planar waveguides of this material [5]. On the other hand, another promising material system that we have developed is based on rare-earth-ion-doped amorphous Al_2O_3 layers grown onto thermally oxidized silicon substrates [6].

2 EXPERIMENTAL

The surface-relief gratings on dielectric channel waveguides were realized by use of a FEI Nova 600 dual-beam FIB machine. The acceleration voltage was set to 30 kV and the milling current was chosen to be either 48 pA or 93 pA. In order to avoid charging of the structures a Cr or Pd/Au layer with a thickness ranging from 10 to 50 nm was sputtered on top of the channel waveguide structures. In order to analyze grating parameters, such as grating depth or sidewall slope, cross-sectioning of the milled structures was performed. Local deposition of a Pt layer on the region where the cross-section profile is to be investigated was performed. Pt was in-situ and locally grown in order to avoid material re-deposition while milling the cross-section. Next, a large hole was milled using a high current of 92 nA. The trench, as shown in Fig. 1, was milled with a sloped angle in order to avoid long milling times. Finally, a polishing

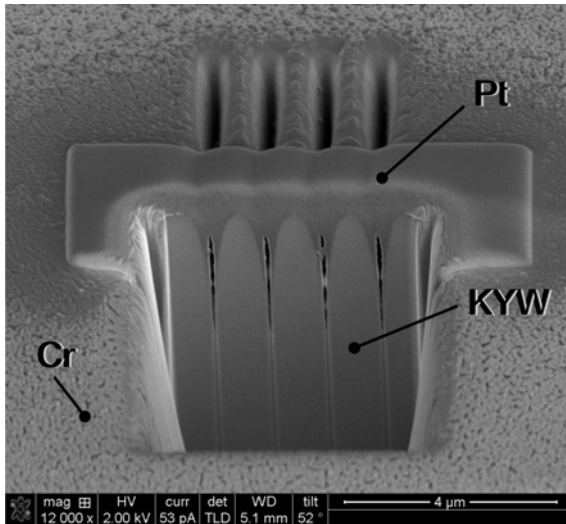


Figure 1: SEM cross section image of a milled Bragg grating on KYW used to assess realized structures.

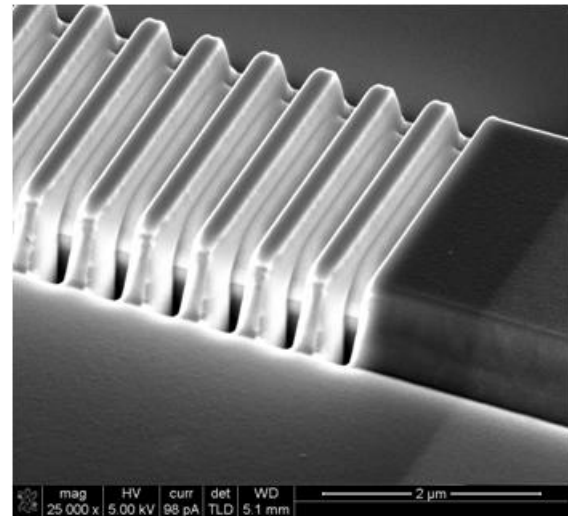


Figure 2: A reflection grating on Al_2O_3 channel waveguide realized by the optimized FIB milling procedure.

process was applied by using a current of 93 pA to facilitate a high contrast image.

The KYW channel waveguides had a 3- μm -thick core layer doped with Gd^{3+} and Lu^{3+} to obtain a refractive index increase of the guiding layer of about 0.015 compared to the undoped KYW substrate. The channel waveguide widths varied between 8 and 6 μm . The etch depth of the channel waveguides was about 1.3 μm . We used Phoenix Opto Designer and Phoenix Field Designer [7] to simulate the optical performance of the gratings and determine the optimum grating dimensions for the available KYW channel waveguides. The milled grating structures had a period of 1.12 μm and a total length of 4.48 μm . In order to avoid charging of the structures, a Pd/Au or Cr metal layer with a thickness of 50 nm was sputtered on top before the milling process.

The thickness of the Al_2O_3 channel waveguides was ~ 550 nm and the grating structures were milled by ~ 200 nm (Fig. 2). The length of each grating was ~ 47.5 μm . Waveguides with widths between 2.8 and 3.4 μm were used.

3 RESULTS AND DISCUSSIONS

3.1 FIB milling of Al_2O_3 grating structures

The gratings were realized using a predefined mask file (stream file) that contains milling time, pixel information, and pixel sequence for the desired geometry. The flexibility provided by the stream-file-based patterning allows us to choose the pathway by which the grating is defined on the waveguide.

It was found that when the scanning is done along a direction perpendicular to the grating grooves, the cross-sectional profile is distorted due to redeposition effects and the inter-groove space is also milled, resulting in “sinking” of the entire grating structure. Moreover, using small dwell times and higher number of loops resulted in smoothing out the effects of redeposition. A successful realization of a reflection grating with optimized milling parameters is depicted in Fig. 2.

3.2 FIB milling optimization for KYW

The initial focus of the experiments was to achieve high milling depths on KYW within a short fabrication time for avoiding any possible drift problems of the focused ion beam. Two ion beam currents of 93 pA and 280 pA were tested. The higher value allowed a shorter milling duration of about 20 minutes in total. Increasing the ion dose per area increased the milling depth as expected. This increase however, was not linear, as the milling depth was

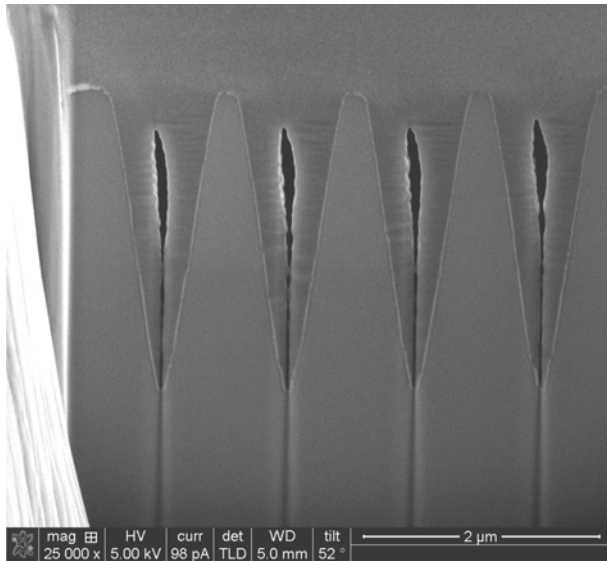


Figure 3: Cross section profiles of Bragg grating in KYW milled without optimization.

strongly affected by re-deposition of material during milling. The gratings were realized using a predefined design mask file, which contains dwell time and pixel sequence for the desired geometry. The dwell time was set to 0.005 ms for the first experiments, while the number of loops and ion current was varied in order to obtain the desired grating depth of 4.3 μm .

The second part of this work focused on diminishing the re-deposition effects during the milling process. The stream-file contains the design of the pathway by which the gratings are milled on the waveguide. A re-distribution of the pixels' location and variation of dwell time was implemented along each grating period. The goal of the experiment was to reduce the re-deposition effects by varying the dwell time per pixel, without increasing the dose per area in order to optimize the milling process for steep sidewalls. The dwell time and pixel resolution increment at the sidewalls was compensated by a loop repetition decrement. The dwell time was varied linearly, with a maximum value at the grating sidewalls to a minimum value at the center. This leads to a higher dose per area near the sidewalls. In an alternative approach, the pixel location was linearly re-distributed such that the pixel density was larger near the sidewalls than in the center.

Both techniques resulted in a reduced re-deposition effect and, therefore, steeper sidewalls compared to the initial "flat" dose distribution. For these experiments the total dose per area was about 33000 $\text{pC}/\mu\text{m}^2$.

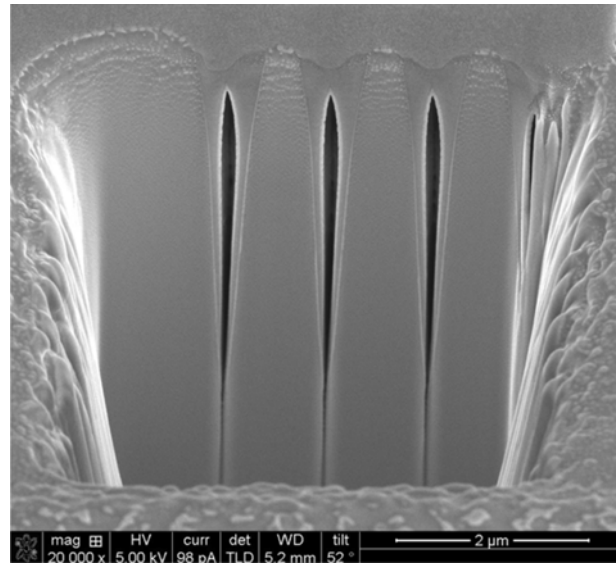


Figure 4: Cross section profiles of Bragg grating in KYW milled with optimized parameters.

Figures 3 and 4 show the cross-section scanning electron microscope (SEM) images of two samples with grating structures. The grating structure of Fig. 3 was milled with a standard stream file without optimization. For the grating structure depicted in Fig. 4 we applied the described optimization processes. The dose per area for this grating was 33000 $\text{pC}/\mu\text{m}^2$. The dwell time was varied between 0.003-0.07 ms. Figure 4 reveals a strong improvement of the total angle between the sidewalls and milling depth increase when applying the dose distribution scheme [3].

4 CONCLUSIONS

An optimization procedure for FIB milling of both, shallow and deep grating structures was developed. Re-deposition effects were significantly reduced and grating structures more than 5 μm in depth, with an improved total sidewall angle of about 5°, were achieved by varying dwell time and pixel resolution distribution for the same dose per area.

This work was supported by the Netherlands Organization for Scientific Research (NWO) through the VICI Grant no. 07207 "Photonic Integrated Structures" and by the European Union, contract IST-NMP-3-017501 (Photonic Integrated Devices in Activated Amorphous and Crystalline Oxides - PI-OXIDE).

REFERENCES

- [1] A. A. Tseng, "Recent developments in nanofabrication using focused ion beams," *Small* 1, 924-939 (2005).
- [2] W. C. L. Hopman, F. Ay, W. B. Hu, V. J. Gadgil, L. Kuipers, M. Pollnau, and R. M. de Ridder, "Focused ion beam scan routine, dwell time and dose optimizations for submicrometre period planar photonic crystal components and stamps in silicon," *Nanotechnology* 18, 195305 (2007).
- [3] F. Ay, I. Iñurrategui, D. Geskus, S. Aravazhi, and M. Pollnau, "Integrated lasers in crystalline double tungstates with focused-ion-beam nanostructured photonic cavities," *Laser Phys. Lett.* 8, in print (2011).
- [4] D. Geskus, S. Aravazhi, K. Wörhoff, and M. Pollnau, "High-power, broadly tunable, and low-quantum-defect $\text{KGd}_{1-x}\text{Lu}_x(\text{WO}_4)_2:\text{Yb}^{3+}$ channel waveguide lasers," *Opt. Express* 18, 26107-26112 (2010).
- [5] D. Geskus, S. Aravazhi, E. Bernhardt, C. Grivas, S. Harkema, K. Hametner, D. Günther, K. Wörhoff, and M. Pollnau, "Low-threshold, highly efficient Gd^{3+} , Lu^{3+} co-doped $\text{KY}(\text{WO}_4)_2:\text{Yb}^{3+}$ planar waveguide lasers," *Laser Phys. Lett.* 6, 800-805 (2009).
- [6] K. Wörhoff, J. D. B. Bradley, F. Ay, D. Geskus, T. P. Blauwendraat, and M. Pollnau, "Reliable low-cost fabrication of low-loss $\text{Al}_2\text{O}_3:\text{Er}^{3+}$ waveguides with 5.4-dB optical gain," *IEEE J. Quantum Electron.* 45, 454-461 (2009).
- [7] Phoenix Software, version 3.0.6 beta, www.phoenixbv.com